Caving 2026 – A van As, D Cumming-Potvin & J Wesseloo (eds)

doi:10.36487/ACG_repo/2645_92

Staged calibration of a cave-scale numerical model for the New Afton C-Zone block cave

Christian Cancino [a,*], Miguel Fuenzalida [a], Yoko Yanagimura [b]

[a] *ITASCA, USA*

[b] *Coeur Mining, Inc, Canada*

Abstract

Numerical models are widely applied in block caving operations to support design and operational decision-making. However, their reliability depends on robust calibration to observed cave behaviour and rock mass response. Calibration remains challenging due to the complex interaction between cave propagation, stress redistribution, rock mass strength, progressive damage and structural controls.

This paper presents a staged calibration methodology applied to a cave-scale numerical model of the C-Zone block cave at the New Afton mine, located at approximately 1,150 m depth. The model was developed in FLAC3D and coupled with MassFlow to assess breakthrough timing into the overlying B3 lift and to simulate upward cave propagation. Initial model assumptions based on previous studies resulted in overprediction of cave propagation and time-domain reflectometry (TDR) cable breakage, highlighting the need for site-specific calibration.

Calibration was undertaken in 2 stages using monitoring datasets including TDR and Geo4Sight measurements. The first stage incorporated a detailed fault catalogue, improving the representation of structural controls on cave propagation and resulting in better agreement with interpreted cave geometry and extent of fractured zone. The second stage refined the mechanical response of the caved material by increasing the minimum Young's modulus of broken rock within IMASS, reducing excessive deformation and improving agreement with observed propagation rates and TDR breakage.

Results indicate that structural controls and the stiffness of the caved material are both key controls on model response in the C-Zone cave. The staged approach provides a transparent and practical framework for calibration, supporting the use of numerical models as effective tools for operational decision-making in block caving.

Keywords: *block caving, numerical modelling, rock mass characterisation, geotechnical monitoring*

1 Introduction

Numerical modelling has become a key tool for supporting design and operational decision-making in block caving. Applications range from forecasting cave propagation and assessing breakthrough potential to managing infrastructure risk and informing production planning. However, the reliability of these models depends on their ability to reproduce observed cave behaviour, which requires appropriate calibration against field data.

Calibration at cave scale remains challenging. Cave propagation is governed by the interaction of stress redistribution, rock mass strength, progressive rock mass damage, gravity-driven flow and structural controls. In this context, progressive damage refers to the gradual degradation of the rock mass strength and stiffness as deformation accumulates beyond peak strength conditions (strain softening behaviour). These processes

* Corresponding author. Email address: ccancino@oneitasca.com

are strongly interdependent and evolve over time, while the rock mass properties that govern them are uncertain to some degree and can vary significantly over relatively short distances, in the order of 10–100 m. As a result, calibration is not a single-step process, but an iterative exercise requiring integration of multiple datasets and progressive refinement of model inputs.

At New Afton mine, previous studies (Cancino et al. 2022, 2024) established a baseline numerical modelling framework for cave-scale assessment using FLAC3D coupled with MassFlow. While this framework successfully captured overall cave behaviour, its application to the C-Zone cave highlighted discrepancies between model predictions and observed response, particularly with respect to cave propagation rate and the extent of rock mass damage over the life of mine.

This paper presents a staged calibration approach developed for the C-Zone block cave. The methodology builds on an initial base case derived from previous studies and progressively incorporates site-specific complexity to improve agreement with monitoring data. Calibration is evaluated against multiple datasets, with particular emphasis on time-domain reflectometry (TDR) breakage data and interpreted cave geometries.

The objective is not only to improve model accuracy, but also to demonstrate how numerical modelling can be applied as a practical operational tool, with transparent assumptions, traceable calibration steps and clearly defined model limitations.

2 Site background and C-Zone overview

The New Afton mine is a porphyry copper-gold deposit located in British Columbia, Canada. The mine comprises multiple cave lifts, with C-Zone representing the deepest block cave development at approximately 1,150 m below surface (Figure 1). C-Zone was initiated using an advanced undercutting sequence, with the undercut front maintained ahead of drawbell construction. As cave construction progressed and the lead-lag distance between the undercut and drawbell fronts increased, the later stages of development became more representative of a pre-undercutting sequence. The first undercut blast was fired in September 2023, and the las undercut rings were fired in June 2025. The first drawbell was blasted at the end of September 2023. Cave construction was completed when the final drawbell was fired in April 2026.

The C-Zone block cave is developed beneath previously mined zones, including the B3 lift, and is characterised by a complex geological and structural setting. The rock mass consists of variably altered volcanic and intrusive units, with strength and deformability influenced by alteration intensity and fracture density (Kamp 2022). In addition to small-scale fabric anisotropy, the rock mass is intersected by a network of faults with varying persistence, orientation and mechanical properties.

Caving in C-Zone is influenced by both rock mass conditions and structural controls, as well as by its interaction with overlying excavations. Understanding the timing of upward propagation, the potential for breakthrough into the B3 lift, and the evolution of cave shape is critical for operational planning and risk management.

A comprehensive cave monitoring program has been implemented in C-Zone to track cave growth and the associated rock mass response. The system includes TDR cables installed in boreholes to detect progressive rock mass damage above the cave, Geo4Sight wireless SMART markers to monitor cave back response through RSSI (received signal strength indication) between adjacent markers and 3-axis tilt measurements from on-board accelerometer based inclinometers with magnetic orientation capabilities, and a microseismic system to track the evolution of the seismogenic zone during cave propagation. Together, these datasets provide complementary constraints on damage development, cave back response and cave growth, forming a strong basis for calibration of the numerical model.

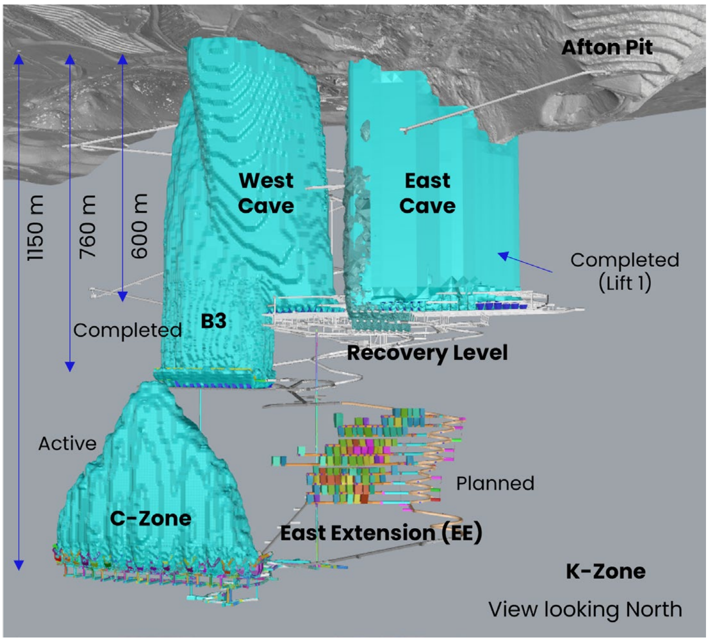

Figure 1 Overview of multiple lifts location at New Afton mine

3 Numerical modelling framework

The numerical modelling approach follows the framework established in previous studies (Cancino et al. 2024), combining FLAC3D (ITASCA 2026a) for rock mass response with MassFlow (ITASCA 2026b) for gravity-driven flow within the cave.

FLAC3D is used to simulate stress redistribution, rock mass damage and cave propagation using a strain softening constitutive model (IMASS). MassFlow is coupled to represent material flow within the cave column, enabling simulation of cave growth, airgap formation and interaction with broken material.

The model geometry is constructed at cave scale using an octree discretisation approach, where a large initial volume is progressively subdivided into smaller zones in areas requiring higher resolution. This approach allows representation of the full C-Zone cave geometry, overlying units including the B3 lift, major structural features where relevant, and reconciled production sequencing and draw strategy, while maintaining computational efficiency at the mine scale. Mine infrastructure, including tunnels, was not explicitly excavated in the model. Instead, infrastructure response was evaluated implicitly by interrogating the model results at the virtual locations of the excavations.

Boundary conditions and initial stresses are defined based on site data and previous calibration work. Rock mass properties are assigned using geotechnical domaining informed by laboratory testing, core logging and empirical relationships.

While this framework provides a robust starting point, its predictive capability depends on calibration to observed behaviour, particularly in relation to cave propagation rate, extent and timing of rock mass damage and the influence of structural features.

4 Baseline model and initial discrepancies

A baseline model was developed using assumptions consistent with previous studies (Cancino et al. 2024), including rock mass properties derived from available datasets (Table 1), implicit representation of major structural features (Figure 2), where fault zones are incorporated as volumetric regions of faulted ground with reduced strength properties (rock block strength of 24 MPa) rather than as explicit discrete surfaces. Default IMASS parameters were adopted to define the ultimate strength of caved rock (Table 2), including a minimum Young's modulus of 100 MPa. A rock density of 2,700 kg/m^3 was used in the model.

Table 1 Peak strength intact rock properties and GSI to derive rock mass properties (Cancino et al. 2024)

Domain	GSI	UCSi (MPa)	m*i*	Ei (GPa)
Picrite	53	56	15	50
Diorite	45	67	20	36
Conglomerate	44	48	15	24
BXF	60	51	20	45
Kamloops	44	48	15	24
Monzonite	55	62	20	47
Ashcroft	45	67	20	36
Faults	44	24	15	24

Notes: GSI – geological strength index; UCSi - uniaxial compressive strength of intact rock samples, m*i* - fundamental material constant, Ei - intact (or Initial) Young's modulus

Table 2 Ultimate strength of caved rock

Domain	m_b	s	a	Rock mass deformation modulus, E_{rm} (MPa)
Caved rock	2.0	0.0	0.85	100

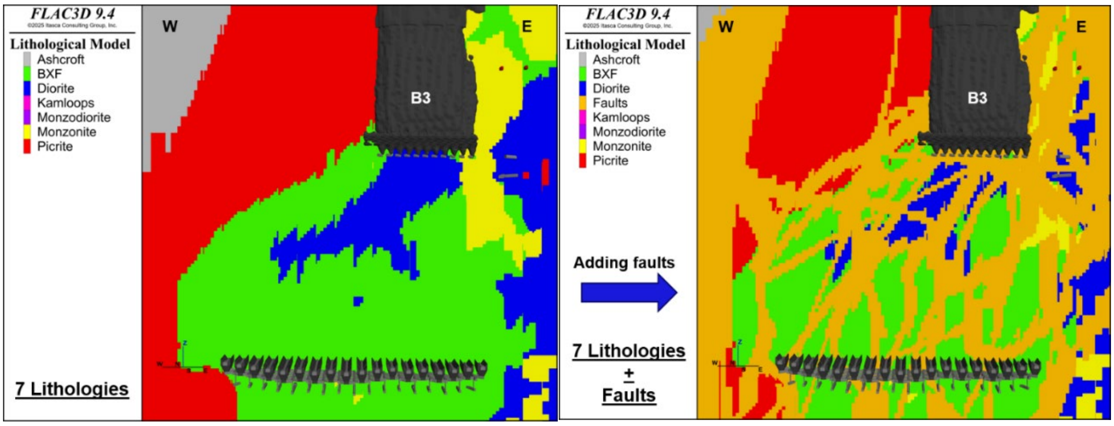

(a) (b)

Figure 2 (a) West–east cross-sections illustrating the lithological units; (b) Resulting units after incorporating the structural model as a separate unit with uniform properties

When applied to the C-Zone cave, the baseline model reproduced general cave propagation behaviour but exhibited important discrepancies when compared to monitoring data. The model overpredicted cave propagation rates, resulting in earlier and more extensive upward cave growth than indicated by observations. In addition, the model overestimated the extent of TDR breakage, suggesting more widespread rock mass damage than had been recorded during monitoring.

To evaluate model performance, the predicted cave response was compared against interpreted cave shapes developed from monitoring data up to October 2025 using 2 independent interpretations (Figure 3). These interpreted cave shapes were developed as approximate bounding interpretations of the cave response, recognising that the available monitoring systems are expected to respond to different stages of caving development. Both interpretations considered the available instrumentation, seismicity overlying the cave back and abutments, and the production profile; however, different weighting was assigned to the Geo4Sight and TDR datasets to reflect whether the interpretation was intended to represent the mobilised cave limit or the broader yielded/fractured zone surrounding the cave. In areas without monitoring data, the production profile, particularly the height of draw, was converted to an interpreted cave height using a multiplier calibrated against areas where downhole instrumentation or probe holes provided direct constraints on cave response.

The first interpretation, referred to as 'NA Conservative', was defined based primarily on areas of full RSSI loss in the Geo4Sight wireless SMART markers, interpreted as complete dislocation from the marker chain. This interpretation was supported by a review of TDR break locations, measured TDR strains and SMART marker tilt; however, these datasets were not used as the primary controls in defining the cave shape. Seismicity was also reviewed to assess whether its spatial distribution was consistent with the overall interpreted cave geometry. This interpretation represents the approximate extent of mobilised cave material and is compared against the model-predicted emergent mobilised limit.

The second interpretation, referred to as 'NA Clips', was defined primarily by the locations of full TDR breakage and was more strongly constrained by the spatial distribution of seismicity because it was intended to represent the broader yielded/fractured zone surrounding the mobilised cave. Less weight was placed on the Geo4Sight markers, although the extent of tilt recorded by the SMART markers was also considered. This interpretation is compared against the model-predicted emergent fracture limit, defined using a total strain criterion of 0.5%.

The comparison highlights that the baseline model overestimates both the upward extent of the mobilised cave and the surrounding fractured zone. These discrepancies indicate that key controlling mechanisms are not being adequately captured. In particular, the assumption of a uniform strength assigned to all modelled faults, based on a rock block strength of 24 MPa, likely overestimates structural connectivity and cave propagation potential throughout the domain. In addition, the inclusion of lower-confidence interpreted faults, some of which may not exist or may have limited persistence, introduces further uncertainty and may contribute to an overestimation of caving rates. The results also suggest that the mechanical behaviour assigned to the caved material within the cave may be too compliant, promoting excessive deformation and upward cave growth relative to observations.

These observations motivated a staged calibration approach in which model complexity was increased progressively to isolate and address the sources of mismatch.

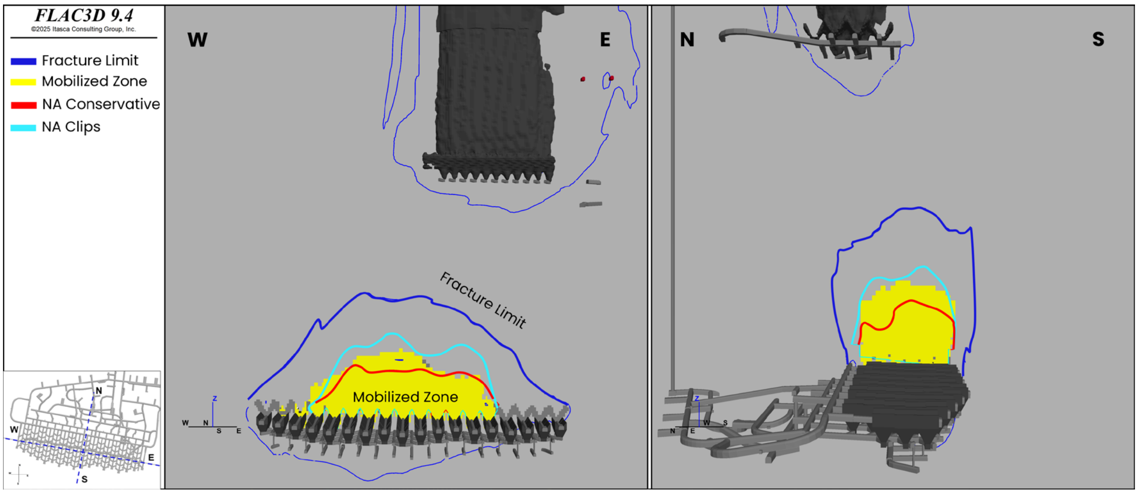

Figure 3 Cross-sections illustrating the baseline model predictions with interpreted cave shapes based on monitoring data by October 2025. Mobilised zone limit (in yellow) is compared with NA Conservative (in red), and emergent fracture limit (in blue) is compared with NA Clips (in cyan)

5 Staged calibration approach

Calibration was performed in stages, progressively introducing site-specific complexity and evaluating its impact on model response. The workflow was designed to first address the dominant controls on cave geometry, followed by refinement of rock mass response within the cave.

5.1 Stage 1: incorporation of fault catalogue

The first stage of calibration, as recommended by Cancino et al. (2024), focused on improving the representation of structural controls through incorporation of a fault catalogue developed by the mine. This catalogue included information on fault confidence, intensity, mechanical characteristics (Is50, Jn, Q′ and RMR_{89}), and supporting geological observations from site.

In contrast to the simplified structural representation adopted in the baseline model (with 36 faults in total), only faults classified as high or moderate confidence (18 faults) were incorporated into the numerical model. These faults were further subdivided into high- and low-intensity categories (Figure 4), with different rock block strengths assigned according to fault intensity (24 MPa and 48 MPa, respectively). This approach allowed the model to better capture localised weakening and deformation along fault zones, directional controls on cave propagation, and more realistic interaction between the cave back and structural features.

The inclusion of the fault catalogue had a first-order effect on model response. Cave propagation became more spatially variable, with localised acceleration or inhibition depending on fault intensity. This resulted in improved agreement with the interpreted cave shapes and a better representation of the observed asymmetry in cave growth.

In addition, the spatial distribution of modelled damage showed improved alignment with TDR breakage data, particularly in zones where faulting was interpreted to influence cave progression. Despite these improvements, the model continued to overpredict the overall extent of damage and propagation rate, indicating that additional refinement was required.

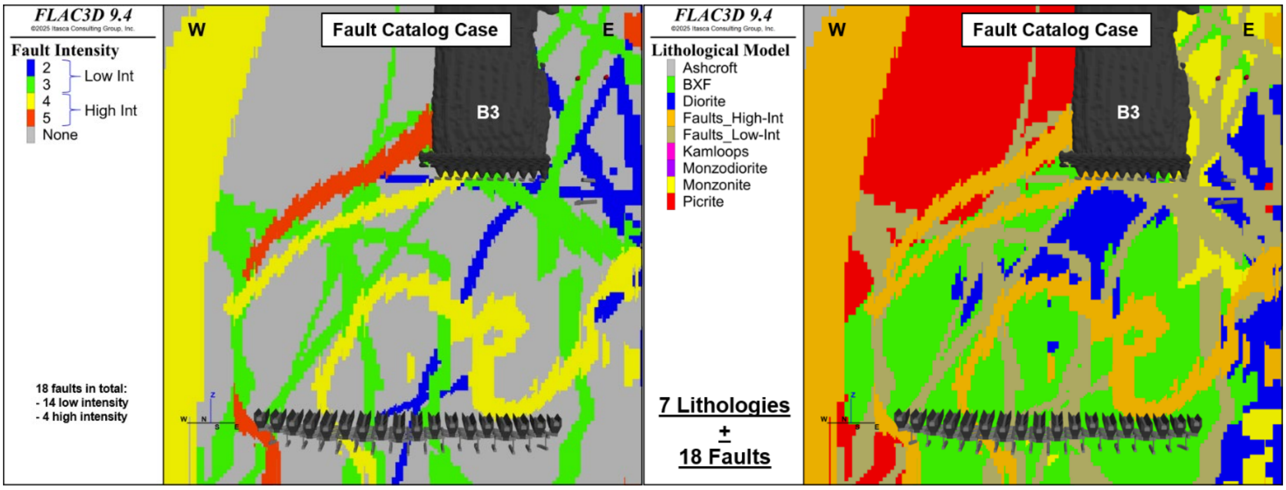

Figure 4 (a) East–west cross-sections illustrating the fault intensity; (b) Resulting lithological units used in the FLAC3D model

5.2 Stage 2: adjustment of caved rock stiffness

The second stage focused on refining the mechanical response of the caved material within the IMASS constitutive model, particularly the stiffness assigned to the caved rock. As a rock mass bulks via shear or tension, it is expected to experience a drop in modulus. The results of laboratory testing by Pappas & Mark (1993) showed that the modulus of rock drops in a nonlinear fashion with increased bulking, and that the rate of modulus change is a function of fragment shape and intact strength. The IMASS model incorporates this modulus change towards a minimum value to which the rock can be degraded.

In the baseline configuration, a default minimum Young’s modulus of approximately 100 MPa was used for caved rock material. This resulted in a highly compliant cave, promoting a more intense stress redistribution and facilitating upward cave propagation beyond what was supported by monitoring data.

To better reflect observed behaviour, the minimum modulus was increased to 500 MPa, representing a stiffer caved rock mass. This adjustment reduces excessive deformation within the cave and limits the rate at which stresses are transferred to the cave back. The increase in minimum modulus of broken rock from 100 to 500 MPa was not intended to represent a directly measured property at New Afton, but rather a calibrated lower-bound stiffness for compacted broken rock within the cave. This adjustment is consistent with published observations indicating that the stiffness of fragmented rock masses is dependent on stress and compaction, increasing as voids close and fragments rearrange (Pappas & Mark 1993). Previous studies on caved and gob material (in longwall mining) have also suggested that the modulus of broken rock masses may range approximately from 1/100 to 1/57 of the intact rock modulus depending on packing conditions (Hsiung & Peng 1985; summarised by Singh & Singh 2011). For intact moduli in the order of 40 GPa, this corresponds to approximately 400–700 MPa, supporting the use of 500 MPa as a plausible calibrated lower-bound value for compacted broken material inside the cave. Nevertheless, the adopted modulus remains a calibrated parameter and should be further constrained with site-specific observations where available. The impact of this modification was twofold. First, cave propagation rates decreased, resulting in improved agreement with the timing of interpreted cave geometries. Second, the extent of modelled damage was reduced, leading to better alignment with TDR breakage observations.

Importantly, this adjustment did not significantly change the cave geometry controlled by structural features but rather moderated the overall system response. This highlights the complementary roles of structural representation and constitutive behaviour in controlling model outcomes.

5.3 Stage 3: calibration against monitoring data

Model predictions were evaluated against monitoring datasets, with emphasis on:

- TDR breakage profiles, providing direct indication of rock mass damage progression
- interpreted cave shapes derived from monitoring and operational data.

The calibrated model showed improved agreement in both the extent and timing of TDR breakage, and the geometry of the cave front (Figure 5).

Remaining discrepancies were assessed in the context of model assumptions and data uncertainty, with calibration focusing on achieving an improved representation rather than an exact replication of the phenomenon.

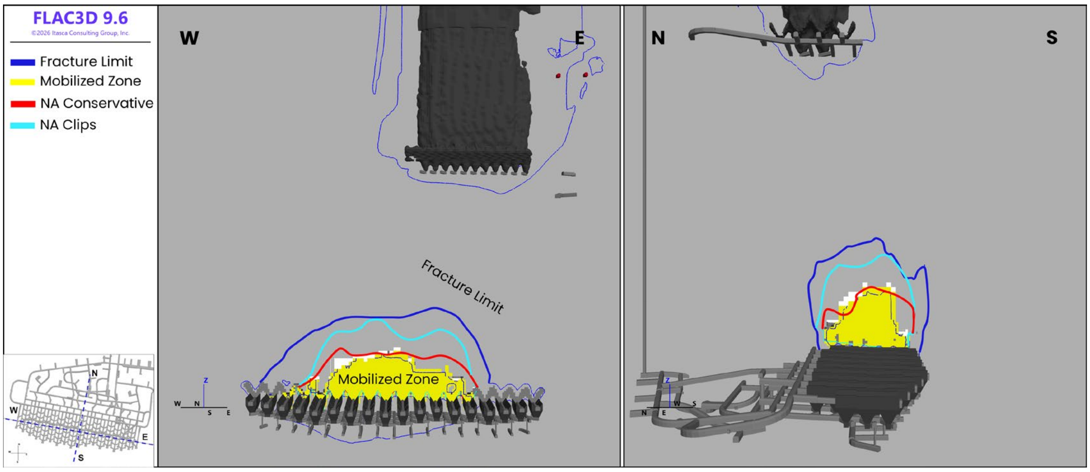

Figure 5 Cross-sections illustrating the calibrated model predictions with interpreted cave shapes based on monitoring data by October 2025. Mobilised zone limit (in yellow) is compared with NA Conservative (in red), and emergent fracture limit (in blue) is compared with NA Clips (in cyan)

6 Results and model performance

The staged calibration approach resulted in a model that more closely matches observed cave behaviour in the C-Zone cave. The combination of increased caved rock stiffness and explicit fault representation reduced the tendency of overpredicting cave propagation. Cave growth became more consistent with site observations, particularly in relation to upward propagation towards the B3 lift.

TDR breakage patterns were also better captured, with the model reproducing the general extent and distribution of damage. Importantly, the calibrated model reflects the localised influence of faults, which act as both facilitators and barriers to propagation depending on their orientation, scale and properties.

To further evaluate model performance with existing instrumentation, model predictions are compared against TDR breakage data for selected boreholes. Figure 6 presents the evolution of breakage for TDR UA23-304, showing the progression of partial and fully clipped segments over time compared against model predictions based on the advancement of the fracture limit. The model reproduces both the onset of damage and the rate of breakage observed in the field, capturing the rapid progression between October and November 2025 (months 20 and 21 of the simulation). This response is representative of the overall agreement observed across multiple TDR installations. However, since the cave is still at an early stage of propagation, the calibration will continue to be reviewed and refined as additional monitoring data become available, and the cave evolves toward breakthrough conditions.

Figure 7 depicts a cross-section along the same TDR, illustrating the lithological units and structural features intersected by the borehole, including zones of high- and low-intensity faulting. The results highlight a marked increase in damage coinciding with interaction between the propagating cave front and a high-intensity fault zone, characterised by a lower rock block strength of 24 MPa. In contrast, low-intensity faults are represented using a higher rock block strength of 48 MPa, calibrated to reflect tunnel-scale behaviour.

These results emphasise the critical role of faults, particularly weaker high-intensity structures, in locally accelerating cave propagation and controlling damage distribution (Figure 8). While similar modelling approaches may be applied at other caves, the higher stress conditions at C-Zone highlight the importance of these features in cave behaviour, requiring more detailed characterisation and representation of fault intensity to achieve reliable calibration.

Overall, the results emphasise that cave behaviour at New Afton is not governed solely by lithology-based rock mass properties, but is strongly influenced by faults, which play a first-order role in controlling cave propagation and damage distribution. However, this does not imply that increasing the number of represented faults necessarily improves the prediction of cave behaviour. Instead, the results highlight that the selection, characterisation and representation of the most relevant structural features are critical to reproducing the observed cave response. Overrepresentation of faults within the model was found to increase cave propagation, resulting in overprediction relative to observations.

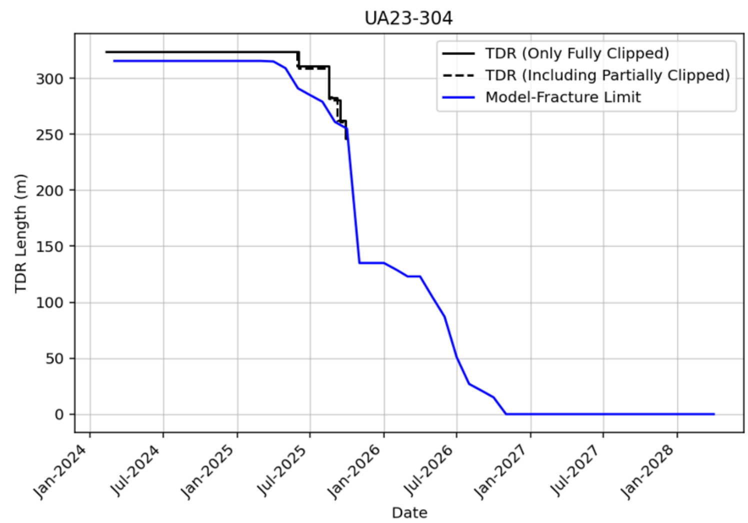

Figure 6 Time-domain reflectometry (TDR) breakage data for UA23-304 TDR from site compared with model predictions of virtual instruments based on emergent fracture limit

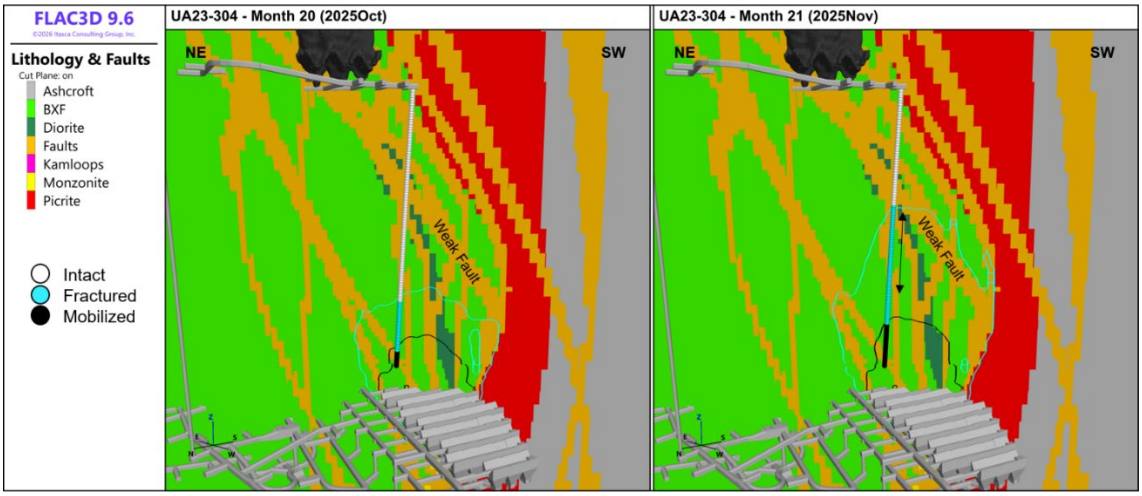

(a) (b)

Figure 7 Cross-sections along UA23-304 time-domain reflectometry illustrating the progress of the emergent fracture and mobilised limits during (a) October 2025; (b) November 2025

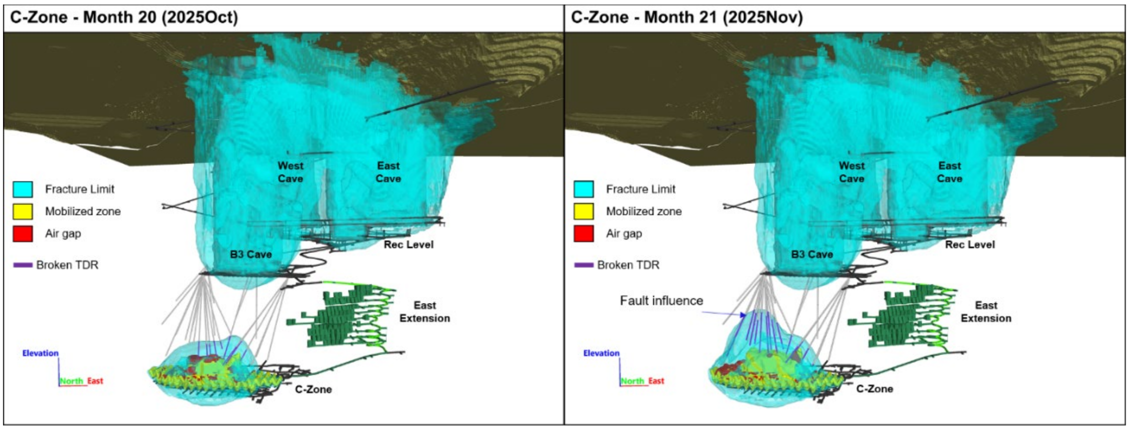

(a) (b)

Figure 8 ISO-view looking north illustrating the cave propagation in terms of fractured and mobilised limits for (a) October 2025; (b) November 2025, where a clear structural influence is observed

7 Discussion: operational use of the model

Numerical models developed for cave mining have significant operational value when they are calibrated against observed cave behaviour and updated as new monitoring data become available. From an operational perspective, a calibrated model provides a defensible basis for decision-making by relating forecast cave behaviour to the observed response of the rock mass under site-specific mining and geological conditions. In the case considered in this paper, the modelling work is specifically focused on the interaction between the C-Zone cave and the overlying B3 level.

In practice, calibrated numerical cave models can be used to assess the timing and likelihood of breakthrough into overlying lifts, support decisions regarding access restrictions and re-entry protocols, and inform the scheduling of closure activities in areas expected to be affected by cave propagation. They can also be used to define the evolving cave geometry, which is critical for evaluating potential airblast scenarios, estimating void configurations, and informing the design basis and location of engineered airblast barricades.

Beyond breakthrough forecasting, calibrated cave models can also be used to evaluate short- and medium-term draw strategies by assessing how different draw patterns may influence cave propagation, cave asymmetry, dilution entry, fines migration and interaction with major structures. This allows operations to test the likely effects of alternative draw approaches before they are implemented in the field, reducing the risk of adverse cave responses and improving alignment between production objectives and geotechnical risk management. The models can also help identify areas of elevated risk associated with structural controls, such as preferential cave deviation into weaker or waste domains, zones susceptible to fines accumulation or remobilisation, and areas where stress redistribution may increase the likelihood of seismic response or ground damage. More broadly, they provide a practical framework for integrating cave back interpretations, seismicity, deformation monitoring, drawpoint performance and geology into a single assessment of cave behaviour, improving confidence in the interpreted cave state and supporting forward-looking operational decisions.

The transparency of the calibration process is equally important. A staged calibration approach makes it easier to understand the influence of key assumptions and input parameters, assess sensitivity to uncertainty, and clearly communicate model limitations to operational stakeholders. This is particularly important in an operating mine, where available datasets are often incomplete and may contain uncertainty, variable quality, or data gaps that require engineering judgement, reasonable assumptions, and a clear strategy for further data collection and analysis. In this context, a transparent and well-calibrated modelling workflow supports more informed, risk-based operational decisions and provides a clear technical basis for communicating the level of confidence that can reasonably be placed in the model results.

8 Conclusion

This study presents a staged calibration methodology for a cave-scale numerical model of the New Afton C-Zone block cave. Starting from a baseline model developed from previous studies, the calibration was progressively refined through adjustment of caved rock stiffness and incorporation of a detailed fault catalogue. These refinements resulted in improved agreement with observed cave behaviour, particularly with respect to cave propagation, interpreted cave geometry, and TDR breakage. The work also shows that calibration at cave scale is inherently iterative, requiring progressive refinement of the model through ongoing interpretation of the geotechnical data available for site characterisation. In this way, the calibration process supports informed refinement of model parameters and key geotechnical assumptions. Overall, the main outcome of the study is not only an improved match to observed behaviour, but also a clearer understanding of the factors controlling cave propagation at C-Zone.

From an operational perspective, the calibrated model provides a more reliable basis for assessing breakthrough into overlying lifts, interpreting cave growth, and supporting decisions related to access restrictions, re-entry protocols, closure planning, and airblast risk management. More broadly, this work demonstrates that when calibration is carried out systematically and tied closely to site observations, cave-scale numerical models can serve as practical tools for risk-informed operational decision-making in block caving. Future development should focus on improved characterisation and spatial integration of key geological controls, including lithology, fault, alteration and rock strength variability through geotechnical block models. New Afton is currently looking to advance systematic point load test campaigns to support the development of spatially distributed Is_{50} block models for future cave-scale simulations.

Acknowledgement

The authors thank the management team at Coeur New Afton for granting permission to publish this work. The New Afton geotechnical team is gratefully acknowledged for their ongoing support and valuable technical discussions throughout the study. The authors also acknowledge Sahar Ghadirianniari for her contributions to the comparison of TDR and model results.

The views and opinions presented in the article are the authors’ own and do not reflect any position or outlook of Coeur New Afton.

References

Cancino, C, Fuenzalida, MA & Kamp, C 2022, 'Modelling considerations for cave compaction at New Afton Mine', in Y Potvin (ed.), *Caving 2022: Proceedings of the Fifth International Conference on Block and Sublevel Caving*, Australian Centre for Geomechanics, Perth, pp. 573–582, https://doi.org/10.36487/ACG_repo/2205_39

Cancino, C, Fuenzalida, M & Kamp, C 2024, 'Numerical modeling of cave propagation and breakthrough timing', in D Johansson & H Schunnesson (eds), *MassMin 2024: Proceedings of the International Conference & Exhibition on Mass Mining*, Luleå University of Technology, Luleå, pp. 548–568, https://doi.org/10.36487/ACG_repo/2435_D-07

Hsiung, SM & Peng, SS 1985, 'First caving and its effects', *Proceedings of the 4th Conference on Ground Control in Mining*, West Virginia University, Morgantown, pp. 83–93.

ITASCA 2026a, *FLAC3D — Fast Lagrangian Analysis of Continua in Three Dimensions*, computer software, version 9.6, Minneapolis, https://itascasoftware.com/products/flac3d/

ITASCA 2026b, *MassFlow — A Gravity Flow Simulator*, computer software, version 9.6, Minneapolis, https://itascasoftware.com/products/massflow/

Kamp, C 2022, 'Management of production drift convergence and redevelopment', in Y Potvin (ed.), *Caving 2022: Proceedings of the Fifth International Conference on Block and Sublevel Caving*, Australian Centre for Geomechanics, Perth, pp. 831–848, https://doi.org/10.36487/ACG_repo/2205_57

Singh, GSP & Singh, UK 2011, 'Assessment of goaf characteristics and compaction in longwall caving', *Mining Technology: Transactions of the Institutions of Mining and Metallurgy: Section A*, vol. 120, no. 4, pp. 222–232, https://doi.org/10.1179/1743286311Y.0000000010

Pappas, D & Mark, C 1993, *Behavior of Simulated Longwall Gob Material, Report of Investigations*, 9458 USBM.